Naunyn-Schmiedeberg's Archives of Pharmacology (2020) 393:1003–1011
https://doi.org/10.1007/s00210-019-01757-5

ORIGINAL ARTICLE

A compartmental approach to isosteviol's disposition in Sprague-Dawley rats

Ayorinde ADEHIN[1,2] · Keai Sinn TAN[1] · Chengjuan ZOU[1] · Zhiqiang LU[1] · Yue LIN[1] · Dongfang WANG[1] · Qing CHENG[3] · Wen TAN[1]

Received: 15 August 2019 / Accepted: 30 October 2019 / Published online: 9 December 2019

Abstract

Isosteviol has been reported to reverse hypertrophy and related inflammatory responses in in vitro models representative of cardiac muscle cells. The disposition of isosteviol is, however, characterized by secondary peaks and long plasma residence time despite reports of a relatively short half-life in liver fractions. The present study describes a compartmental approach to modelling the secondary peaks characteristic of isosteviol's concentration-time data in Sprague-Dawley rats. Oral (4 mg/kg) and intravenous (4 mg/kg) doses of isosteviol were administered to male and female Sprague-Dawley rats. Plasma samples collected between 0 and 72 h, and total bile secreted in 24 h, were analysed for isosteviol content with LC-MS/MS techniques. The disposition of isosteviol was, thereafter, described with a structural model that accounted for the sampling, liver and biliary secretion compartments, with a gap-time characterizing the accumulation and subsequent emptying of isosteviol for re-absorption. The half-life of isosteviol following oral dosing was about 103% greater in female rats than in the male, and the model-derived area under the concentration-time curve (AUC) in 72 h was about 756% greater in female animals than in males. Following the administration of intravenous doses of isosteviol, half-life and AUC in 24 h were about 332% and 595%, respectively, higher in female rats than in males. Isosteviol equivalent secreted into bile over 24 h accounted for about 94% of orally administered dose in male rats, and about 59% of oral dose in females. These findings show a differential systemic removal of isosteviol in Sprague-Dawley rats, likely explainable by gender-related differences in the glucuronidation-capacity of isosteviol.

Keywords Isosteviol · Enterohepatic recycling · Hypertrophy · Pharmacokinetics · Inflammation

Introduction

The reversal of cardiac hypertrophy and related inflammatory responses, in vitro, by isosteviol has been replicated in models by several authors (Wang et al. 2018; Fan et al. 2017; Yang et al. 2018; Tang et al. 2018; Liu et al. 2018; Yin et al. 2017; Hu et al. 2016; Ullah et al. 2019). Isosteviol, responsible for this pharmacological effect, is mainly biotransformed into its acyl-β-D-glucuronide in man and rat. Additional metabolites identified to have been generated from minor metabolic routes included dihydroisosteviol (also reported to exhibit some activity of isosteviol (Wonganan et al. 2013)), mono- and

✉ Wen TAN
went@gdut.edu.cn

Ayorinde ADEHIN
ayoadehin@yahoo.com

Keai Sinn TAN
keaisinn@hotmail.com

Chengjuan ZOU
zeocin@163.com

Zhiqiang LU
luzq85@163.com

Yue LIN
916333547@qq.com

Dongfang WANG
556620x@163.com

Qing CHENG
chengqinghappy@163.com

[1] Institute of Biomedical and Pharmaceutical Sciences, Guangdong University of Technology, Guangzhou, China

[2] Department of Pharmaceutical Chemistry, Faculty of Pharmacy, Obafemi Awolowo University, Ile-Ife, Nigeria

[3] Dermatology Hospital, Southern Medical University, Guangzhou, China

dihydroxy-isosteviol (Adehin et al. 2019; Jin et al. 2010). Jin and colleagues (Jin et al. 2008) described a bi-exponential pharmacokinetic profile of isosteviol in rats, suggesting the significant contribution of a secondary compartment to its disposition. The non-compartmental approach utilized for the estimation of pharmacokinetic parameters by Jin et al. (Jin et al. 2008), however, appeared to have covered the first 12 h only. Half-life, from this study, was estimated at between 1 and 4 h following oral and intravenous doses in rats.

Preliminary studies (in-house) of the pharmacokinetics of isosteviol by our research group, however, noted the persistence of multiple peaks accompanied with quantifiable amounts of isosteviol in the plasma of rats beyond 12 h. This observation appeared consistent with the concentration-time curve presented by Jin et al. (Jin et al. 2008) whose plot did not suggest a rapid terminal decline in the plasma level of isosteviol at 12 h. Zhu et al. (Zhu et al. 2016), hypothesizing a staggered intestinal absorption of isosteviol, utilized a rat-isolated everted gut sac model to assess the differential absorption of isosteviol in the intestinal tract. The study, however, observed no significant difference in the absorption of isosteviol along the duodenum, jejunum, ileum and colon.

Multiple peaks in the concentration-time profile of several xenobiotics are well documented. This phenomenon has been explained as resulting from an interplay of the physicochemical properties of such drugs and their absorption processes, or as a result of enterohepatic recycling of drug molecules among other possible mechanisms (Davies et al. 2010). The present study hypothesizes that enterohepatic recycling of isosteviol underpins its multiple peaking with inferences drawn from (i) the findings of Zhu and colleagues (Zhu et al. 2016) which observed no varied absorption of isosteviol at different intestinal sites, (ii) the dominance of the glucuronidation pathways (Adehin et al. 2019; Jin et al. 2010) for which a release of free isosteviol from its glucuronide by intestinal microbiota, once secreted in bile, appears plausible and (iii) the notable occurrence of isosteviol's secondary peak at regions well beyond the absorption phase. The present study, hence, explored a compartmental model approach, accounting for the recirculation of isosteviol via biliary secretion, in the description of isosteviol's disposition in rats.

Materials and methods

Chemicals

Isosteviol, ethylenediaminetetraacetic acid (EDTA), LC-grade methanol and acetonitrile were purchased from Sigma (Steinheim, Germany). Ammonium acetate, formic acid, dichloromethane, hexane and ethyl acetate were supplied by Macklin Biochemical Co. Ltd. (Shanghai, China). C-19 ethyl ester of isosteviol (Fig. 1, purity > 97%) was synthesized, in-house, by the esterification of isosteviol using ethyl bromide, potassium hydroxide and dimethyl sulfoxide at room temperature for 5 h as earlier described by Zhang et al. (Zhang et al. 2012). Dihydroisosteviol (synthesized by reacting isosteviol with sodium borohydride in methanol at room temperature for 4 h) and the sodium salt of isosteviol were also synthesized in-house. Stock solutions of isosteviol and its C-19 ethyl ester derivative (internal standard) were prepared in LC-grade methanol. Male human liver microsomes (HLM), reduced nicotinamide adenine dinucleotide phosphate (NADPH)-regenerating system, alamethicin, Tris-HCl buffer and $MgCl_2$ were purchased from Corning Inc. (NY, USA). Uridine 50-diphosphoglucuronic acid (UDPGA) was from Sigma (Steinheim, Germany).

Animals

Study approval was granted by the local ethics committee of the Sun-Yat-sen University, Guangzhou, China. Male and female Sprague-Dawley rats were purchased from the Experimental Animal Center of the Guangzhou University of Chinese Medicine (Guangzhou, China). These study animals were housed in cages at about 22 °C for 3 weeks on a 12 h/12 h light/dark cycle with adequate access to food and water.

Study design

Pharmacokinetics of isosteviol following oral and intravenous doses

All animals were fasted overnight and subsequently allowed access to food and water after drug administration. A stock solution for the oral dose in the study animals was prepared by dissolving isosteviol in ethanol: distilled water (50:50) at 70 °C, followed by cooling to room temperature to obtain a clear solution at 27 °C. Oral doses of isosteviol (4 mg/kg), in 200-μL final volumes (< 5% ethanol after further dilution with distilled water), were administered through a gavage to 8 rats (4 males, body weight = 352.75 ± 17.86 g; 4 females, body weight = 242.00 ± 4.55 g). Intravenous doses of isosteviol (as its sodium salt, 4 mg/kg isosteviol equivalent), prepared in normal saline (250-μL final volume), were also administered to another set of 8 rats comprising 4 males (body weight = 284.00 ± 8.49 g) and 4 females (body weight = 253.50 ± 9.19 g). Thereafter, 500 μL of whole blood was drawn at several time points, between 0 and 72 h, into EDTA bottles after drug administration. Samples were processed for plasma within 30 min of collection by centrifugation at 10,000× *g* for 10 min, and stored at − 80 °C until analysis.

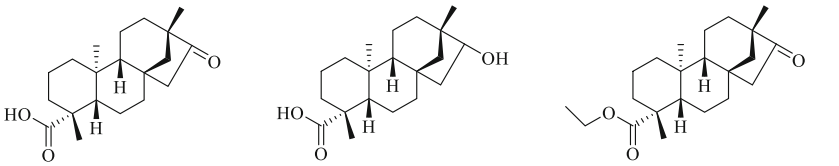

Fig. 1 The structures of isosteviol, dihydroisosteviol and the C-19 ethyl ester of isosteviol

Bile duct cannulation study

Sprague-Dawley rats (2 males, body weight = 295.00 ± 7.07; 2 females, body weight = 249.00 ± 9.90) were anaesthetized, and their bile duct cannulated as described by Tønsberg et al. (Tonsberg et al. 2010). Oral doses of 4 mg/kg isosteviol (prepared as previously described) were administered to animals, and the total bile liberated in 24 h was collected. Samples were stored at − 80 °C until analysis.

Plasma and bile sample preparation for the analysis of isosteviol and its acyl-β-D-glucuronide

One hundred microlitre of plasma, spiked with 10 μL of the internal standard (C-19 ethyl ester of isosteviol, 550 μg/L), was extracted with 1 mL of dichloromethane:hexane:ethyl acetate (ratio 4:4:2) with vortex-mixing for 1 min. The mixture was centrifuged at 10,000× *g* for 5 min, the organic phase aspirated and dried at 50 °C under vacuum. The extracted analytes were subsequently re-dissolved in 110 μL of 90% methanol, vortex-mixed for 30 s and further incubated for 30 min at 50 °C to ensure complete solution of analytes. This was followed by vortex-mixing for another 30 s, and a brief centrifugation for 1 min at 10,000× *g*. The final supernatant was, thereafter, collected for analysis.

To quantify the isosteviol acyl-β-D-glucuronide in bile samples, 1 μL of bile was diluted to 1 mL with LC-grade methanol and vortex-mixed for 2 min. The mixture was then centrifuged at 20,000× *g* for 10 min, and the supernatant collected. Ten microlitre of this supernatant was further diluted to 1 mL with LC-grade methanol. A 100-μL aliquot of the new dilution was spiked with 10 μL of the internal standard, acyl-β-D-glucuronide of dihydroisosteviol (final concentration 22 μg/L), and analysed. The acyl-β-D-glucuronides of isosteviol and dihydroisosteviol were synthesized as previously described by Adehin et al. (Adehin et al. 2019).

Chromatography analysis

A Xevo TQ-S mass spectrometer (Waters, Milford, MA, USA) connected to an ACQUITY UPLC system (Waters, Milford, MA, USA) via an electrospray ionization interface was utilized. To quantify isosteviol in rat plasma, data was acquired from the mass spectrometer in the positive mode by monitoring transitions of m/z 319.22/273.22 (cone voltage 20 V, collision energy 13 eV) for isosteviol, and m/z 347.25/319.26 (cone voltage 10 V, collision energy 15 eV) for the internal standard (C-19 ethyl ester of isosteviol). In bile samples, a transition of m/z 493.24/317.21 (cone voltage 5 V, collision energy 38 eV) was monitored for isosteviol acyl-β-D-glucuronide while m/z 495.26/319.22 (cone voltage 10 V, collision energy 40 eV) was monitored for its internal standard (dihydroisosteviol acyl-β-D-glucuronide) in the negative mode. Source and desolvation temperatures were set at 150 °C and 500 °C, respectively.

Isosteviol and its internal standard in plasma were resolved with an ACQUITY BEH C18 column (3.0 × 50 mm i.d.; 1.7-μm particle size; Waters, Milford, MA, USA) at 40 °C following a 5-μL injection of samples from an autosampler at 15 °C. The mobile phase comprised solvent A (5 mM ammonium acetate and 0.1% formic acid in distilled water) and solvent B (methanol:acetonitrile, 2:8) pumped through the column in a gradient over a 10-min period, at a flow rate of 0.3 mL/min, after a 5-μL sample injection. An effective separation of analytes was achieved by initially pumping a 50:50 ratio of solvents A and B through the column for 5 min followed by a switch to 15:85 ratio of solvent A:solvent B for 1 min. Solvent B then accounted for 95% of the mobile phase for the next 0.8 min, followed by a return to 50% till the 10th minute of the entire run. The chromatographic analysis was validated according to the FDA recommendations (US FDA 2018). Plasma contents of isosteviol were deduced from a calibration curve constructed between 5 μg/L and 1500 μg/L.

Isosteviol acyl-β-D-glucuronide and internal standard in bile was resolved with same column, injection volume, column and sample temperature conditions described for isosteviol. The mobile phase, however, comprised 5 mM of ammonium acetate and methanol pumped through the column in gradient over 10 min. A calibration curve ranging between 0.15 μg/L and 35 μg/L was constructed for quantification.

Data analysis

The empirical model proposed as an explanation for multiple peaking of isosteviol due to enterohepatic recycling was based on the earlier works of Steimer et al. (Steimer et al. 1982), and modified as presented in Fig. 2. Drug delivery and measures of drug concentration in plasma were designated to have occurred in the central compartment, while the removal of

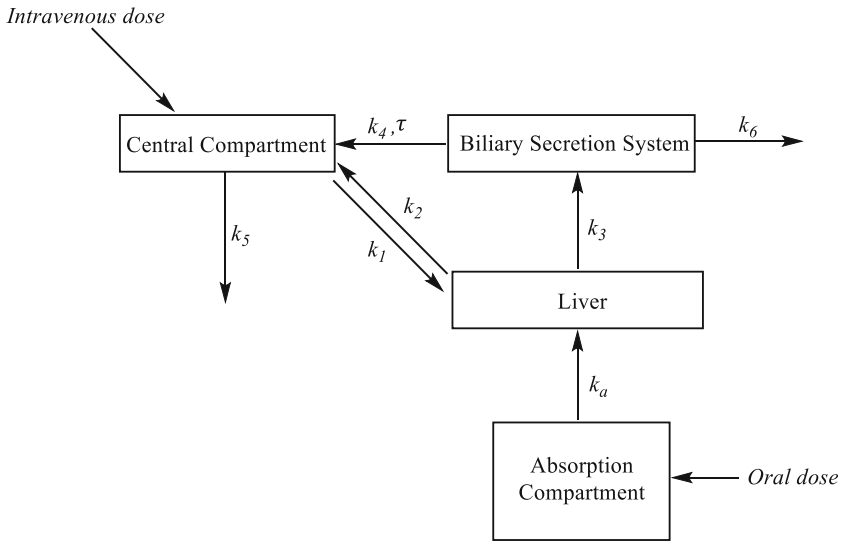

Fig. 2 A schematic representation of the disposition of isosteviol in Sprague-Dawley rats

isosteviol from the systemic circulation occurred from the 'central' and the 'biliary secretion' compartments.

Further, with glucuronidation of isosteviol as the major metabolic pathway (Adehin et al. 2019), the contribution of other routes of metabolism to the systemic loss of isosteviol was assumed to be insignificant. Hence, a gap-time (τ) was inserted between the 'biliary secretion compartment' and 'central compartment' to account for an accumulation of unmetabolized isosteviol or isosteviol's glucuronide. It was assumed that a subsequent hydrolysis of glucuronidated isosteviol was total, and that all free isosteviol molecules were completely emptied back into the central compartment at intervals τ.

Processes of absorption (oral dose), distribution and elimination were assumed to be first-order. The amount of isosteviol administered and absorbed 'A_{abs}' into systemic circulation alongside fraction of drug absorbed 'F' was characterized by a concentration 'C_{cen}', volume of distribution 'V' and a rate constant k_a. The 'biliary secretion system' and 'liver' are characterized by drug amounts A_{bile} and A_{liver}, respectively. Differential equations describing the changes in isosteviol content of the different compartments are as shown in Eq. (1)–(3).

$$\frac{dC_{cen}}{dt} = k_2 \cdot A_{liver} + k_4 \cdot A_{bile\ (t-\tau)} - (k_1 + k_5) \cdot C_{cen} \cdot V \quad (1)$$

$$\frac{dA_{liver}}{dt} = k_a \cdot F \cdot A_{abs} + k_1 \cdot C_{cen} \cdot V - k_3 \cdot A_{liver} \quad (2a, oral dose)$$

$$\frac{dA_{liver}}{dt} = k_1 \cdot C_{cen} \cdot V - k_3 \cdot A_{liver} \quad (2b, intravenous dose)$$

$$\frac{dA_{bile}}{dt} = k_3 \cdot A_{liver} - (k_4 + k_6) \cdot A_{bile\ (t-\tau)} \quad (3)$$

The differential equations describing the structural model were implemented in MATLAB (MATLAB 2018). Model parameters were estimated with lsqnonlin nonlinear least squares optimisation function. Analytical solutions to the model's differential equations were derived using the Laplace transformation in order to optimize curve fitting, and relative standard errors for derived parameters were computed as described by Landaw et al. (Landaw and DiStefano 3rd 1984).

A total elimination rate of isosteviol was assumed, and hence, k_{e_total} was derived as a sum of k_5 and k_6. The half-lives of isosteviol following oral and intravenous doses were then computed using the relation $T_{1/2} = 0.693/k_{e\_total}$. The area under the concentration-time curve (AUC), as predicted by the model was estimated as earlier described by Shepard et al. (Shepard et al. 1985).

Results

Bioanalysis

Peak resolution and linearity of detector response were achieved between 5 μg/L and 1500 μg/L with corresponding retention times for isosteviol and the internal standard being 6.47 min and 7.22 min. Deviations from nominal values of the back calculated concentration of the calibration samples were ≤ ± 6.18%, and assay limits of detection and quantification were 3.78 μg/L and 11.44 μg/L, respectively. Intra-assay impression of the method, expressed as % coefficient of variation (% CV) and studied in six-concentration replicates each at 15 μg/L, 200 μg/L and 1000 μg/L, varied between 2.80% and 9.85%. Similar studies of inter-assay variation had impressions ranging between 2.16% and 10.01%. The assay's relative recovery of isosteviol from plasma matrix varied between 93.82% and 102.54%.

The effect of sample matrix on analyte response was minimal with enhancements of 3.53% at 15 ng/mL, 0.98% at

200 μg/L, and 1.02% at 1000 μg/L. Samples with concentrations exceeding the upper limit of the calibration curve were diluted 1:50 with distilled water. Quantifications resulting from such dilutions in plasma spiked with 1500 μg/L, 5000 μg/L, 10,000 μg/L and 20,000 μg/L isosteviol were characterized by assay impressions (expressed as % CV) that ranged between 0.64% and 3.61%. Accuracy of quantification after sample dilution varied between 100.39% and 101.34%.

Pharmacokinetics of isosteviol in rats

Plots of concentration-time data of isosteviol, following oral and intravenous doses, in male and female rats are shown in Figs. 3 and 4. Pharmacokinetic parameters derived from the model-fitting (Figs. 5, 6) of isosteviol's concentration-time data in rats are presented in Tables 1 and 2. From experimental data, peak plasma concentration (C_{max}) of 3861.24 ± 1560.65 μg/L was reached in 1.31 ± 0.85 h (T_{max}) after oral administration of isosteviol in male rats, while corresponding values for C_{max} and T_{max} in female animals were 14,082.87 ± 4803.52 μg/L and 2.13 ± 1.18 h. The removal of isosteviol from the central compartment following oral and intravenous doses in male and female rats was markedly different with corresponding decreases of about 92% and 89% in the elimination rate constant k_5. While the volume of distribution (V_d) in the central compartment was about 74% higher in male rats than in the females following oral dosing, comparable values of V_d were observed following intravenous administration of isosteviol. Fraction of drug absorbed varied between 60% and 65% in both sexes of rats, and elimination of isosteviol through the biliary secretion system was predicted by the model. The elimination half-life and the AUC derived from parameters generated by the pharmacokinetic model are presented in Table 3.

Isosteviol equivalent in bile as isosteviol acyl-β-D-glucuronide

The amount of isosteviol excreted in bile as isosteviol acyl-β-D-glucuronide within 24 h of oral dosing were 1.16 and 1.09 mg isosteviol equivalent in male rats, and 0.54 and 0.52 mg isosteviol equivalent in female rats. These values amounted to 93.45 ± 4.34% of the administered dose in male rats, and 59.24 ± 1.63% of the administered isosteviol dose in female rats.

Discussion

Previous studies of isosteviol's fate in perfused rat liver, rat liver fraction and human liver fractions had reported the dominance of glucuronidation in its systemic removal. A bile to liver distribution ratio of 6.0 in rat was observed, and terminal half-lives of 13.4 min and 24.9 min, in vitro, in rat and human liver, respectively, were reported (Adehin et al. 2019; Jin et al. 2010). However, disposition kinetic studies of isosteviol in rats, both from a previous study (Jin et al. 2008) and the present study, had suggested significantly longer plasma residence time following non-compartmental analyses of concentration-time data.

The obvious need for a new approach to the description of isosteviol's disposition necessitated the implementation of a unique structural model which accounted for the xenobiotic's recycling through the bile, in vivo. This disposition model, implemented in the present study, showed that the in vivo terminal half-life of isosteviol, while comparable with previous in vitro values in liver fractions, was gender-dependent in rats. In addition, model-predicted values of overall exposure were greater in female rats than in male rats.

Enterohepatic recycling (EHC) of xenobiotic describes processes of (i) absorption of orally ingested substances through the alimentary tract into portal venous blood of enterocytes or the intravenous entry of xenobiotic into systemic blood circulation, (ii) subsequent removal of such substances from blood by uptake into hepatocytes, (iii) secretion of these substances or their metabolites into bile for deposition into the intestinal lumen and (iv) the re-absorption of these substances (or their regenerated form after the enzymic modification of their metabolites) by intestinal cells to start these

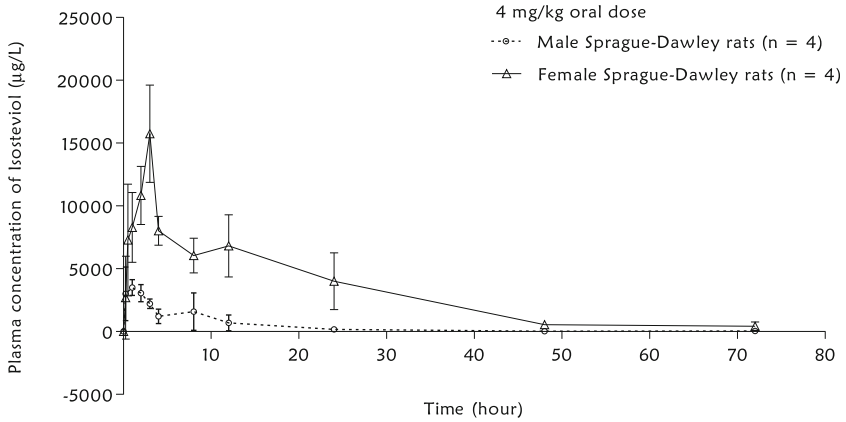

Fig. 3 Plots of the concentration-time data following the oral administration of 4 mg/kg isosteviol in Sprague-Dawley rats. Errors bars are standard deviations from the mean at each data point

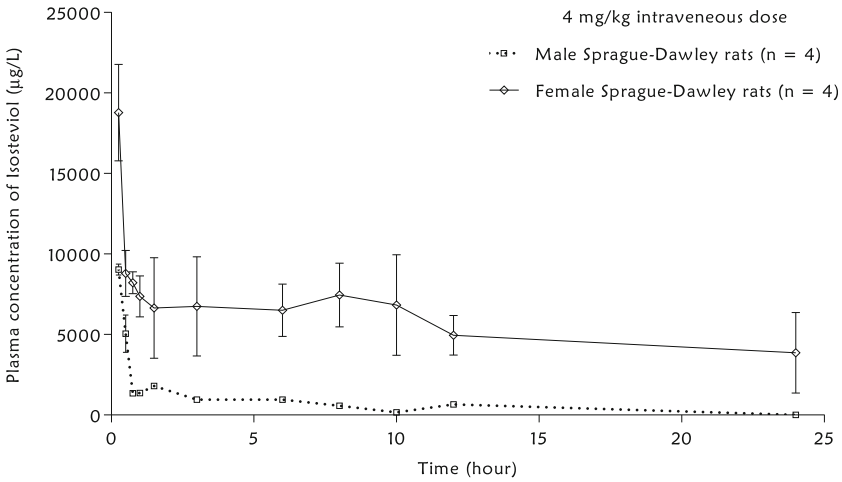

Fig. 4 Plot of the concentration-time data following the intravenous administration in Sprague-Dawley rats at 4 mg/kg isosteviol doses. Errors bars are standard deviations from the mean at each data point

processes all over (Roberts et al. 2002). The described recycling of xenobiotic often results in concentration-time data showing multiple peaks with attendant distortion of disposition parameters of terminal half-lives, area under the time-concentration curve, and estimated bioavailability.

The failure of conventional and simple non-compartmental analysis of concentration-time data to adequately estimate disposition parameters by accounting for the multiple peaking due to EHC had resulted in the utilization of compartmental models which accommodated the biliary secretion and re-absorption of such xenobiotics (Wajima et al. 2002). A few drugs for which EHC has been modelled and studied include lorazepam (Herman et al. 1989), meloxicam (Lehr et al. 2009) and piroxicam (Tvrdonova et al. 2009). Several authors had since devised compartmental approaches implementing gap-times to create delay in the transfer of such xenobiotics from bile compartment to plasma/sampling compartment, and thereby explaining the occurrence of secondary peaks in concentration-time profiles (Steimer et al. 1982; Shepard et al. 1985; Dahlstrom and Paalzow 1978; Pedersen and Miller 1980; Colburn 1984; Funaki 1999).

In the present study, processes of biliary re-circulation modelled as a delay between the bile compartment (biliary secretion compartment, Fig. 2) and the plasma compartment (central compartment, Fig. 2) provided an explanation for the long systemic residence time of isosteviol. The study hypothesis is further supported by a previously established rapid hepatic metabolism of isosteviol in rat liver (Jin et al. 2010), and the over 90% of isosteviol recovered in male rat bile (apparently reflecting the full effect of hepatic first-pass metabolism) which would have made detection at 72 h post-dose impossible in the absence of a re-circulation.

Disposition rate parameters estimated from the present model, however, suggested significant gender-related differences in rats. The longer half-lives of oral and intravenous doses of isosteviol observed in female rats are likely results of a differential hepatic expression of the specific glucuronidating enzyme for isosteviol in this species. On the strength of data available in the present study, it appears that the rate and efficiency of glucuronidation of isosteviol to produce isosteviol acyl-β-D-glucuronide are higher in male rats than in females. Similar gender-related variations in glucuronidation of xenobiotics have been reported with the 5,6-dimethylxanthenone-4-acetic acid (Zhou et al. 2002), emodin (Liu et al. 2010), and *p*-nitrophenol (Catania et al. 1995) in rats. A recent study of the differential expression of uridine

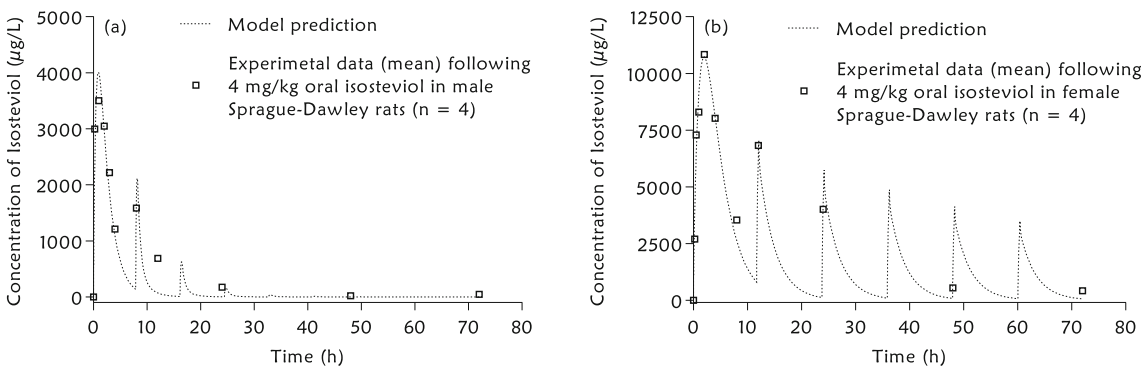

Fig. 5 Plots of the experimental data vs model prediction following oral administration of isosteviol in Sprague-Dawley rats. **a** Model predictions vs average data points from experimental data after the oral administration of isosteviol in male rat. **b** Model predictions vs average data points from experimental data after the oral administration of isosteviol in female rats

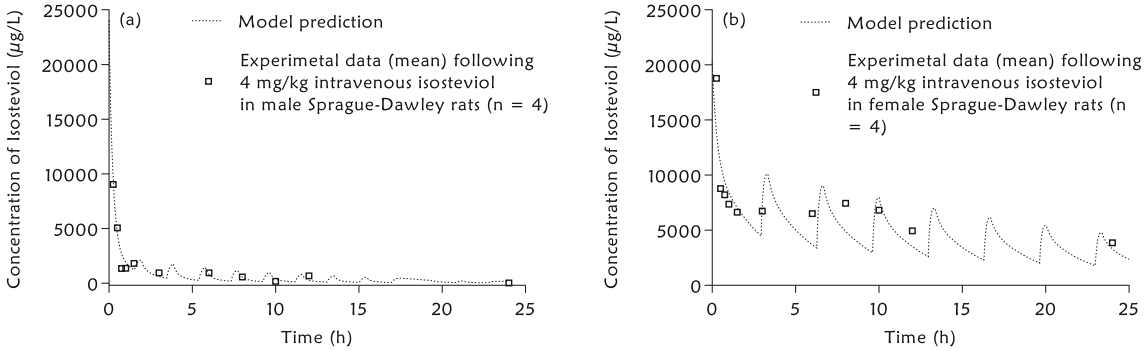

Fig. 6 Plots of the experimental data vs model prediction following intravenous administration of isosteviol in Sprague-Dawley rats. **a** Model predictions vs average data points from experimental data after the intravenous administration of isosteviol in male rat. **b** Model predictions vs average data points from experimental data after the intravenous administration of isosteviol in female rats

5′-diphospho-glucuronosyltransferases (UGTs), the family of enzymes responsible for the glucuronidation of xenobiotics in biological systems, did affirm the differential expression of UGT isoenzymes in rat tissues (Kutsukake et al. 2019). A particular finding of interest for the present study was the report of Kutsukake and colleagues (Kutsukake et al. 2019) which showed that male Sprague-Dawley rats differentially expressed the *UGT2B6* at levels of about 77% higher in male rats than in female. It, however, remains to be determined if the UGT2B6 isoenzyme solely mediates the glucuronidation of isosteviol in Sprague-Dawley rats.

Another observation of interest in the present study was the gender-relation differences in modelled gap-time between the bile compartment and the central compartment. Estimated gap-time, τ, was about 48% greater in female rats than in males after oral dosing (Table 1), and about 92% greater in females than in rats after intravenous dosing (Table 2). In addition, τ values were larger with oral doses (7.9–11.7 h) than they were with intravenous doses (1.5–2.9 h). Since the model utilized assumed an accumulation of xenobiotic in the bile compartment over a time gap followed by a complete emptying into the central compartment, processes of bile production and flow would be expected to impart on estimated values of τ.

Cooks et al. (Cook et al. 1950) did study the role of gender, body and tissue weight on the basal flow of bile in rats. Values of 0.00347 L/h/kg body weight and 0.0099 L/h/100 g liver were reported, and no evidence of gender-induced differences was noted. The gender differences observed in the present study may, hence, be a result of the marked difference in body weight of male (oral dose 352.75 ± 17.86 g; intravenous dose 284.00 ± 8.49 g) and female (oral dose 242.00 ± 4.55 g; 253.50 ± 9.19 g) rats used for the study. While the marked differences in τ for oral and intravenous doses are unknown at this time, it is likely that a complex interplay between the time required for oral absorption and a unique interaction of isosteviol salt with bile transport components might be responsible.

Table 1 Compartmental model-derived pharmacokinetic parameters of isosteviol after oral dosing in Sprague-Dawley rats

	Oral dose (4 mg/kg isosteviol)	
Pharmacokinetic parameters	Male rats ($n = 4$)	Female rats ($n = 4$)
k_a (h^{-1})	1.35 [7.140]	1.038 [9.955]
Biliary CM time lag, τ (h)	7.981 [0.225]	11.600 [2.845]
Volume of distribution, V (L)	0.0562 [30.205]	0.0276 [8.993]
Fraction of drug absorbed, F	0.648 [10.924]	0.605 [6.471]
k_1 (h^{-1})	0.521 [33.973]	3.653 [78.401]
k_2 (h^{-1})	0.766 [3.394]	2.909 [80.062]
k_3 (h^{-1})	0.752 [139.894]	0.302 [3.642]
k_4 (h^{-1})	3.527 [116.501]	1.762 [45.687]
Central CM elimination rate, k_5 (h^{-1})	0.413 [55.448]	0.028 [489.285]
Biliary CM elimination rate, k_6 (h^{-1})	0.336 [3.309]	0.341 [95.200]

Square brackets are standard error values expressed in %; *CM*, compartment

Table 2 Compartmental model-derived pharmacokinetic parameters of isosteviol after intravenous dosing in Sprague-Dawley rats

	Intravenous dose (4 mg/kg isosteviol)	
Pharmacokinetic parameters	Male rats ($n = 4$)	Female rats ($n = 4$)
Biliary CM gap-time, τ (h)	1.528 [4.427]	2.938 [1.062]
Volume of distribution, V (mL)	0.0473 [12.825]	0.0496 [8.054]
k_1 (h^{-1})	3.071 [11.304]	1.732 [37.913]
k_2 (h^{-1})	0.521 [51.468]	1.586 [69.104]
k_3 (h^{-1})	0.601 [62.170]	0.535 [44.204]
k_4 (h^{-1})	0.740 [90.493]	5.448 [35.191]
Central CM elimination rate, k_5 (h^{-1})	0.827 [40.867]	0.0905 [46.481]
Biliary CM elimination rate, k_6 (h^{-1})	0.364 [97.857]	0.185 [247.086]

Square brackets are standard error values expressed in %; *CM*, compartment

Table 3 Model-derived estimates of elimination half-life and area under the concentration-time curve for isosteviol in 16 Sprague-Dawley rats

Pharmacokinetic parameters	Male ($n = 4$) 4 mg/kg oral dose	Female ($n = 4$)
Half-life (h)	0.925	1.878
$AUC_{0–72\ h}$ (h*μg/L)	15,568.879	131,948.877
	4 mg/kg intravenous dose	
Half-life (h)	0.582	2.515
$AUC_{0–24\ h}$ (h*μg/L)	17,073.146	118,714.298

AUC,'Area under the concentration-time curve' derived from the fitting of the final compartmental model describing the disposition of isosteviol in Sprague-Dawley rats

Half-life ($T_{1/2}$) = 0.693/k_{e_total} where k_{e_total} is the sum of k_5 and k_6

Parameters were derived using model-predicted estimates

* implies multiplication

Conclusions

The modelled-disposition of isosteviol with a consideration for its enterohepatic recycling in Sprague-Dawley rats exhibited marked gender-related differences in terminal half-life and overall exposure. Plasma residence of isosteviol was longer in female rats than in male rats.

Authors' Contributions WT and AA conceived and designed the work. AA, KST, CZ, ZL, YL, DW and QC contributed to the acquisition, analysis or interpretation of data for the work with the guidance of WT. All authors drafted the work or revised it critically for important intellectual content and approved the final version of the manuscript.

Funding information This work was supported by the National Science and Technology Major Projects for "Major New Drugs Innovation and Development" (Grant Number 2019ZX09301120) and the Science and Technology Innovation Project of Foshan (Grant Number 2017IT100162).

Compliance with ethical standards Study approval was granted by the local ethics committee of the Sun-Yat-sen University, Guangzhou, China.

References

Adehin A, Tan KS, Lu Z, Cheng Q, Tan W (2019) In vitro metabolic stability and biotransformation of isosteviol in human and rat liver fractions. Drug Metab Pharmacokinet 34:194–200

Catania VA, Dannenberg AJ, Luquita MG, Sanchez Pozzi EJ, Tucker JK, Yang EK, Mottino AD (1995) Gender-related differences in the amount and functional state of rat liver UDP-glucuronosyltransferase. Biochem Pharmacol 50(4): 509–514

Colburn WA (1984) Pharmacokinetic analysis of concentration-time data obtained following administration of drugs that are recycled in the bile. J Pharm Sci 73(3):313–317

Cook DL, Beach DA, Bianchi RG, Hambourger WE, Green DM (1950) Factors influencing bile flow in the dog and rat. Am J Phys 163(3):688–694

Dahlstrom BE, Paalzow LK (1978) Pharmacokinetic interpretation of the enterohepatic recirculation and first-pass elimination of morphine in the rat. J Pharmacokinet Biopharm 6(6):505–519

Davies NM, Takemoto JK, Brocks DR, Yanez JA (2010) Multiple peaking phenomena in pharmacokinetic disposition. Clin Pharmacokinet 49(6):351–377

Fan Z, Lv N, Luo X, Tan W (2017) Isosteviol prevents the prolongation of action potential in hypertrophied cardiomyoctyes by regulating transient outward potassium and L-type calcium channels. Biochim Biophys Acta Biomembr 1859(10):1872–1879

Funaki T (1999) Enterohepatic circulation model for population pharmacokinetic analysis. J Pharm Pharmacol 51(10):1143–1148

Herman RJ, Van Pham JD, Szakacs CB (1989) Disposition of lorazepam in human beings: enterohepatic recirculation and first-pass effect. Clin Pharmacol Ther 46(1):18–25

Hu H, Sun X, Tian F, Zhang H, Liu Q, Tan W (2016) Neuroprotective effects of Isosteviol sodium injection on acute focal cerebral ischemia in rats. Oxidative Med Cell Longev 2016:1379162

Jin H, Gerber JP, Wang J, Ji M, Davey AK (2008) Oral and i.v. pharmacokinetics of isosteviol in rats as assessed by a new sensitive LC-MS/MS method. J Pharm Biomed Anal 48(3):986–990

Jin H, Wang J, Gerber JP, Davey AK (2010) Disposition of isosteviol in the rat isolated perfused liver. Clin Exp Pharmacol Physiol 37(5–6): 593–597

Kutsukake T, Furukawa Y, Ondo K, Gotoh S, Fukami T, Nakajima M (2019) Quantitative analysis of UDP-Glucuronosyltransferase Ugt1a and Ugt2b mRNA expression in the rat liver and small intestine: sex and strain differences. Drug Metab Dispos 47(1):38–44

Landaw EM, DiStefano JJ 3rd (1984) Multiexponential, multicompartmental, and noncompartmental modeling. II. Data analysis and statistical considerations. Am J Phys 246(5 Pt 2): R665–R677

Lehr T, Staab A, Tillmann C, Trommeshauser D, Schaefer HG, Kloft C (2009) A quantitative enterohepatic circulation model: development and evaluation with tesofensine and meloxicam. Clin Pharmacokinet 48(8):529–542

Liu W, Tang L, Ye L, Cai Z, Xia B, Zhang J, Hu M, Liu Z (2010) Species and gender differences affect the metabolism of emodin via glucuronidation. AAPS J 12(3):424–436

Liu Q, Hu H, Hu T, Han T, Wang A, Huang L, Tan Q, Tan W (2018) STVNa attenuates right ventricle hypertrophy and pulmonary artery remodeling in rats induced by transverse aortic constriction. Biomed Pharmacother 101:371–378

MATLAB (2018) 9.4. Natick M: The MathWorks Inc. Available at: www.mathworks.com

Pedersen PV, Miller R (1980) Pharmacokinetics of doxycycline reabsorption. J Pharm Sci 69(2):204–207

Roberts MS, Magnusson BM, Burczynski FJ, Weiss M (2002) Enterohepatic circulation: physiological, pharmacokinetic and clinical implications. Clin Pharmacokinet 41(10):751–790

Shepard TA, Reuning RH, Aarons LJ (1985) Estimation of area under the curve for drugs subject to enterohepatic cycling. J Pharmacokinet Biopharm 13(6):589–608

Steimer JL, Plusquellec Y, Guillaume A, Boisvieux JF (1982) A time-lag model for pharmacokinetics of drugs subject to enterohepatic circulation. J Pharm Sci 71(3):297–302

Tang SG, Liu XY, Ye JM, Hu TT, Yang YY, Han T, Tan W (2018) Isosteviol ameliorates diabetic cardiomyopathy in rats by inhibiting ERK and NF-kappaB signaling pathways. J Endocrinol 238(1):47–60

The United States Food and Drug Administration (2018). Bioanalytical method validation guidance for industry. Available at: https://www.fda.gov/regulatory-information/search-fda-guidance-documents/bioanalytical-method-validation-guidance-industry

Tonsberg H, Holm R, Bjerregaard TG, Boll JB, Jacobsen J, Mullertz A (2010) An updated and simplified method for bile duct cannulation of rats. Lab Anim 44(4):373–376

Tvrdonova M, Dedik L, Mircioiu C, Miklovicova D, Durisova M (2009) Physiologically motivated time-delay model to account for mechanisms underlying enterohepatic circulation of piroxicam in human beings. Basic Clin Pharmacol Toxicol 104(1):35–42

Ullah A, Munir S, Mabkhot Y, Badshah SL (2019) Bioactivity profile of the diterpene isosteviol and its derivatives. Molecules 24(4)

Wajima T, Yano Y, Oguma T (2002) A pharmacokinetic model for analysis of drug disposition profiles undergoing enterohepatic circulation. J Pharm Pharmacol 54(7):929–934

Wang M, Li H, Xu F, Gao X, Li J, Xu S, Zhang D, Wu X, Xu J, Hua H, Li D (2018) Diterpenoid lead stevioside and its hydrolysis products steviol and isosteviol: biological activity and structural modification. Eur J Med Chem 156:885–906

Wonganan O, Tocharus C, Puedsing C, Homvisasevongsa S, Sukcharoen O, Suksamrarn A (2013) Potent vasorelaxant analogs from chemical modification and biotransformation of isosteviol. Eur J Med Chem 62:771–776

Yang Y, Yang J, Zhang H, Mo C, Zhou T, Tan W (2018) The investigation of protective effects of isosteviol sodium on cerebral ischemia by metabolomics approach using ultra-high-performance liquid chromatography coupled with quadrupole time-of-flight tandem mass spectrometry. Biomed Chromatogr:e4350

Yin C, Chen Y, Wu H, Xu D, Tan W (2017) Attenuation of ischemia/reperfusion-induced inhibition of the rapid component of delayed rectifier potassium current by Isosteviol through scavenging reactive oxygen species. Biochim Biophys Acta Biomembr 1859(12):2447–2453

Zhang T, Lu LH, Liu H, Wang JW, Wang RX, Zhang YX, Tao JC (2012) D-ring modified novel isosteviol derivatives: design, synthesis and cytotoxic activity evaluation. Bioorg Med Chem Lett 22(18):5827–5832

Zhou S, Kestell P, Tingle MD, Paxton JW (2002) Gender differences in the metabolism and pharmacokinetics of the experimental anticancer agent 5,6-dimethylxanthenone-4-acetic acid (DMXAA). Cancer Chemother Pharmacol 49(2):126–132

Zhu J C-jZ, Yu Z-t, Xie S-l, Tan W (2016) Study on the absorption characteristics of isosteviol by rat isolated everted gut sacs. Chinese Journal of New Drugs 25(22):2637–2640